ENGINEERING PRACTICE OF GEOTHERMAL RECHARGE TECHNOLOGY FOR LELING SANDSTONE THERMAL STORAGE

by

Hongyan LI [a,b*], ***Jiangfeng WANG*** [a], ***Bin LIU*** [a,b], ***and Pengtao WANG*** [a,b]

[a] School of Energy and Power Engineering, Xi'an Jiaotong University, Xi'an, China
[b] Sinopec Green Energy Geothermal Development Co., Ltd, Xianyang, China

Original scientific paper
https://doi.org/10.2298/TSCI221003213L

Geothermal well recharge is one of the main measures to maintain the production capacity of geothermal field, and sandstone reservoir recharge is a very difficult work. Taking the Leling area as an example, the permeability, porosity, throat characteristics and rock mechanical properties of sandstone thermal reservoirs were studied to clarify the main geological controlling factors that affecting the recharge of sandstone thermal reservoirs. The numerical simulation model of "one mining one irrigation" geothermal development system is established to study its heat transfer characteristics. The results show that the physical properties and water quality characteristics of sandstone thermal reservoir in Leling area meet the sandstone recharge conditions. The larger the distance between the mining and filling wells is, the longer the time required for the thermal breakthrough of the mining wells is, and the smaller the variation range of the mining temperature is. When the reinjection volume of the reinjection well is 65 m³ per hour, the reasonable well spacing with the production well is about 300 m. When the horizontal well distance is constant, with the increasing of flow, geothermal water connection time is faster, the average porosity >30%, the average permeability >1100 mD, the average cumulative thickness of sand layer is greater than 195 m is more conducive to geothermal tail water recharge. In geothermal reinjection field test, the reinjection rate is 100%, the maximum reinjection volume is 82 m³ per hour and reinjection operation is stable.

Key words: *sandstone thermal reservoir, geothermal well, recharge capacity, reservoir physical properties*

Introduction

Geothermal energy is a non-polluting, renewable and clean energy. Compared with traditional fossil energy, it has the advantages of large reserves, wide distribution and high energy utilization rate. However, over exploitation or improper conservation of geothermal resources will lead to depletion of resources. In order to ensure the sustainable development of geothermal resources and avoid environmental pollution, the most effective technical measure is geothermal recharge technology [1-4]. Reinjection is a reinjection method of geothermal water into the geothermal reservoir section through geothermal reinjection wells [5-7]. Reinjection cannot only solve the problem of geothermal wastewater, but also improve or restore the heat production capacity of geothermal reservoirs, which maintain the fluid pressure of geothermal reservoirs, and maintain the continuous exploitation and recycling of geothermal fields [8-10]. The establishment

* Corresponding author, e-mail: lihongyan@stu.xjtu.edu.cn

of heat extraction system is one of the most important ways to develop geothermal. However, geothermal recharge is one of the important problems restricting the technology, especially the recharge of sandstone strata is more complicated. In 1969, the USA Cysers geothermal field recharge project opened the prelude to geothermal recharge. So far, the recharge of tail water from sandstone thermal reservoir is still a worldwide problem. Many scholars have studied the recharge of geothermal tail water. For example, McDowell-Bover [11] divided the source of suspended matter into two types, one is the solid particles carried by the recharge water itself, and the other is the solid particles generated inside the aquifer under hydrodynamic or hydrochemical effects. The large particulate matter precipitated and aggregated in the infiltration medium, and the main location was on the surface of the infiltration zone. Due to the temperature, pressure, bacteria and water compatibility of minerals in hot water, the precipitation of various salts in geothermal water has become a common concern in porous geothermal reservoir recharge [12]. In terms of recharge blockage mechanism, Juerg *et al.* [13] discussed the distribution of silica, and concluded that the main source of silicate scale in geothermal water exploitation and recharge process is amorphous silica, especially aluminum-containing amorphous silica. Wang *et al.* [14] proposed the influence of geothermal abandoned water recharge layer, recharge amount and recharge on the seepage field and temperature field of thermal reservoir. According to Xianyang reinjection test well and the reinjection experience, the mechanism and feasibility of reinjection evaluate the economic benefits of reinjection of mining well and reinjection well, and obtains a reasonable balance mode of mining and reinjection [15]. Zarrouk *et al.* [16] proposed to divide the recharge area into infield recharge and outfield recharge according to the connectivity between injection and production wells. Stein *et al.* [17] studied the migration and evolution of aluminosilicate minerals in thermal reservoir environment. Xu and Pruess [18] simulated the mineral scaling caused by hot water recharge in fractured geothermal fields. Rivera *et al.* [19] have shown that the impact of recharge on production depends on factors such as its thermal state, geological structure, and hydrological environment, and have evaluated recharge systems for thermal reservoir characteristics. Settari [20] used a variety of methods to study the coupling of geothermal water recharge. Microorganisms (mainly bacteria) in common recharge water sources usually have strong environmental adaptability [21]. During the recharge process, the bacteria and their metabolites attach and accumulate on the surface of the aquifer medium and at the pore throat, which reducing the effective porosity of the medium and causing aquifer blockage [22]. The traditional microbial culture technology is insufficient to simulate the spatial environment and nutritional conditions of microbial survival, and a large number of microorganisms are unculturable. This technology is limited in the study of groundwater microorganisms [23]. Knowles *et al.* [24] proposed that biofilm formation will accelerate the occurrence of medium blockage. Thullner *et al.* [25] found that extracellular polymers produced by bacterial metabolism were the main reason for the decrease of permeability.

Aiming at the difficult problem of sandstone thermal reservoir recharge, the permeability, porosity, throat characteristics, rock mechanics and other characteristics of mountain rock thermal reservoir in Leling area were studied. Through numerical modelling analysis, the main control factors affecting the recharge performance of sandstone thermal reservoir were clarified, and field test verification was carried out to provide guidance for sandstone thermal reservoir recharge.

Thermal reservoir geological analysis

Regional geological structure of MSH well

The sedimentary environment is stable, and the Neogene sandstone thermal reservoir without water-blocking fault is favorable for recharge. Leling City is a part of North China

Plain. This area belongs to Ningjin-Qingyun uplift (IV) area, a secondary tectonic unit of North China Platform (I), Liao-Ji Platform syncline (II), and Chengning uplift (III). The eastern and southeastern parts are adjacent to Wudi bulge, the western and northern parts are adjacent to Ningjin bulge, and the southern part is Huimin sag, which constitute the basic outline of regional basement structure.

Leling City is located in the Cenozoic fault basin. Due to the influence of Yanshan movement and Himalayan movement, it has been slowly declining and deposited a huge thick Cenozoic stratum. As shown in tab. 1, the Paleogene is lacustrine clastic sedimentary rock, containing gypsum, the thickness changes greatly, the sedimentary thickness is more than 1500~3000 m. The thickness of Neogene is relatively stable, which is a fluvial-lacustrine deposit, with a bottom depth of 1350~1650 m. The thickness of Quaternary plain group is relatively stable, which is alluvial, alluvial-lacustrine and marine sediments, and the burial depth is 160~300 m. According to the cuttings logging, drilling time (speed) logging and comprehensive logging data, combined with the comparative analysis of regional geological data. The

Table 1. Lithologic characteristics of Leling stratum

Rock stratum and its symbols	Buried depth of top and bottom plates [m]	Thickness [m]	Brief description of lithology	Characteristics of thermal reservoir
Cenozoic quaternary (Q)	0~513	513	It is mainly fluvial sedimentary stratum. The upper part of the lithology is sandy clay, clayey sand, silt mixed with silt, and the lower part is gravel, gravelly coarse sand, clay and sandy clay interbedding	Quaternary stratum is loose and not cemented, and there are many sand layers and gravelly sand layers
Minghuazhen formation of Neogene (N_2m)	513~1050	537	The upper part of the lithology is mainly composed of brown red, brown yellow and greyish green mudstone, sandy mudstone, interbedded with light yellow fine sandstone in unequal thickness, and the bottom is gravelly coarse sandstone	Degree of formation cementation is also low, and the borehole wall is prone to collapse and block falling, which makes it difficult to maintain the borehole wall
Neogene Guantao Formation [N_2g]	1050~1420	370	Purple red, gray green, brown yellow mudstone and sandy mudstone are brittle and well cemented. Light yellow, gray white medium fine sandstone, coarse sandstone, interbedded with unequal thickness. The bottom is gravelly coarse sandstone, thick	There is a small amount of gypsum in the Neogene Guantao formation, and the mud has a large water loss. It is very easy to reduce the diameter and stick to the drill. It is difficult to drill
Paleogene Shahejie Formation (E_3S)	1420~1530	110.61	It is mainly grayish green, grayish blue, brownish grey, purplish red mudstone and sandy mudstone. It is brittle and tightly cemented. It is in non-waiting interbedding with grayish green, brownish Grey Marl and calcareous mudstone. There is also a small amount of grayish white calcareous mudstone, which is tightly cemented.	

geothermal water wells drilling through the strata from new to old in this study area are quaternary plain group, neogene minghuazhen group, guantao group and shahejie group.

Sandstone geothermal reinjection

Through the research and field test of sandstone geothermal reinjection, the porosity, permeability, sand thickness and channel radius are the main physical factors affecting sandstone economic reinjection. The preliminary conclusions are shown in tab. 2.

Table 2. Parameter table of rechargeable strata in the study area

Region	Average porosity [%]	Average permeability [md]	Average sand layer thickness [m]	Average hole roar radius [μm]	Result
North China Plain	>25	>500	>150	>3	Beneficial to reinjection
Large Intermountain Basin	>20	>250	>250	>3	Beneficial to reinjection

Thermal reservoir properties

As shown in fig. 1, the study area is centered on the MSH recharge well. In the northeast and southeast directions of the recharge wells, the DD and MSH mining wells in the Didu Garden are distributed, respectively. The distances from the MSH recharge wells are 423 m and 192 m, respectively. The vertical depth of MSH recharge well is 1418.46 m (the inclined depth is 1530.61 m). The thermal reservoir aquifer is mainly the Neogene Guantao Formation, and the Shahejie Formation aquifer is less. The main recharge layer of MSH recharge well is the Neogene Guantao Formation. The depth of thermal reservoir is between 1199.69 m (inclined depth) and 1420.30 m (inclined depth). The thickness of single layer is 22.6~56.3 m, a total of 5 layers, and the cumulative aquifer thickness is 194.71 m. The porosity of sandstone aquifer used is 36.77~40.95%, and the permeability is generally $1839.8 \cdot 10^{-3}$ μm^2 to $2771.1 \cdot 10^{-3}$ μm^2.

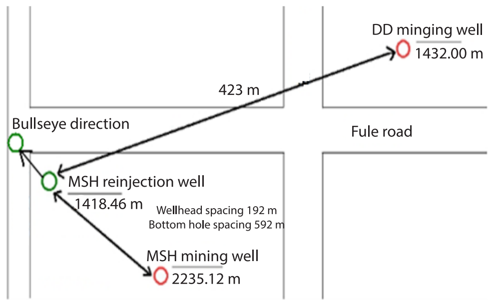

Figure 1. Location distribution map of irrigation and mining wells in irrigation area

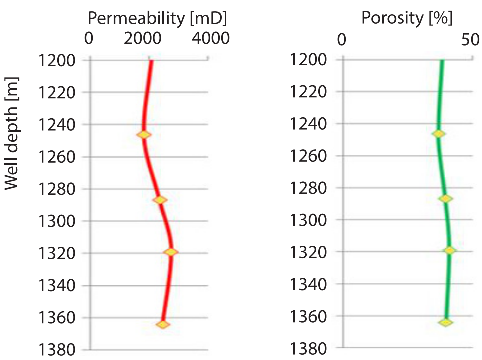

Figure 2. Leling MSH well porosity and permeability distribution map

The Neogene Guantao Formation (N_2g) in the study area is the main thermal reservoir of thermal storage fluid and the main water-intaking section of irrigation and production wells in the irrigation area. The formation thickness of this group is generally 142~380 m, and the sand thickness ratio is 25.92~40.95%. According to the statistics of porosity and permeability data reported by well completion, the physical parameters of irrigation and production wells in the recharge area are shown in tab. 3.

Table 3. Physical parameters of each well in back irrigation area

Well name	Main thermal reservoir	Thermal reservoir depth [m]	Single layer thickness [m]	Number of layers	Cumulative thickness [m]	Porosity [%]	Permeability [$10^{-3}\mu m^2$]
MSH Reinjetion well	Neogene Guantao Formation, Sandstone thermal reservoir in Shahejie Formation	1199.69~ ~1420.30	22.6~56.3	55	194.71	36.77~ ~40.95	1839.8~ ~2771.1
MSH Mining well	Neogene Guantao Formation, Shahejie Formation, Sandstone thermal reservoir in Kongdian Formation	1226.25~ ~2115.72	1.40~50.65	118	191.55	7.44~ ~41.73	7.95~ ~41.85

The logging data of geothermal wells in Leling MSH well and its surrounding areas are counted. Combined with the physical property analysis results of field rock samples, the average porosity and permeability of the target layer in Leling MSH well area are shown in fig. 2. The average porosity is greater than 30%, the average permeability is greater than 1100 mD, and the average cumulative thickness of sand layer is greater than 195 m. Combined with the results of tail water recharge of MSH well in two heating seasons, it is beneficial to geothermal tail water recharge under the physical properties of reservoir.

Reservoir rock composition analysis

For the mineral composition and content of the blank core of MSH recharge well, the blank core is X-ray diffracted, and the experimental results are shown in fig. 3 and tab. 4. The main minerals of geothermal reservoir core in recharge well are quartz, plagioclase, potassium feldspar and calcite. Among them, aluminosilicate minerals dominated by quartz and potassium feldspar account for 70.2%, carbonate minerals dominated by calcite account for 22.3%, and clay minerals account for 6%.

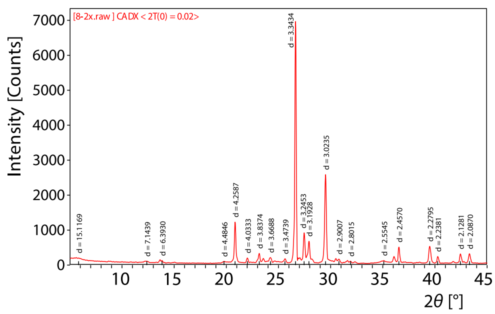

Figure 3. The X-ray diffraction pattern of Leling MSH core

Table 4. The X-ray diffraction results of core, backwater scale and suspended solids in recharge wells

Sample	Quartz	Plagioclase	Potash feldspar	Calcite	Iron dolomite	Montmorillonite	Pyrite	Siderite	Kaolinite
Core	45.1	11.8	13.3	21.0	1.3	4.0	–	–	2.0

Core mechanical properties

The experimental cores were taken from the Upper N_2g thermal reservoir sandstone with a depth of 1200 m in the recharge well of Leling. The porosity is between 36.77% and 40.95%, and the permeability is between $1839.8 \cdot 10^{-3}$ μm^2 and $2771.1 \cdot 10^{-3}$ μm^2. In this experiment, the core is cut into three sections according to the ratio of height to diameter (2 : 1), and the uniaxial compressive strength is 0.054 MPa, 0.065 MPa, and 0.11 MPa, respectively under natural conditions. The weighted average uniaxial compressive strength of the core is

0.076 MPa. The core is coarse sandstone, unequal thickness interbedded, loose, cannot be tensile and shear strength test. Generally, the compressive strength of sandstone is between 11~252 MPa, and the average compressive strength is 75 MPa. The average uniaxial compressive strength of the core is only 0.076 MPa.

Core pore throat characteristics

The experimental cores were taken from the thermal reservoir sandstone of the Upper N_2g at a depth of 1200 m in the MSH recharge well in Leling. As shown in tab. 5, the maximum pore throat radius were 73.3 μm, 35.636 μm, 72.817 μm, and 72.817 μm, the average pore throat radius were 4.486, 3.176, 4.472, 4.548.

Table 5. Determination results of core pore throat

Place name	Sample	Maximum throat radius [μm]	Average throat radius [μm]
Shan Dong (MSH)	8-2-1	73.300	4.486
	8-2-2	35.636	3.176
	1-1	72.817	4.472
	1-2	72.817	4.548

Water chemical properties of thermal storage fluid

Through the indoor water chemical analysis and field verification of Leling MSH well, the same layer recharge can effectively reduce the probability of chemical blockage, and the different water quality recharge in different layers increases the probability of chemical blockage and reduces the recharge effect.

In the other area, the piper diagram, as shown in fig. 4, of water chemistry of thermal reservoir fluid shows that the main cations of all wells are Na^+, the anions of MSH recharge wells are mainly Cl^-, followed by SO_4^{2-}, and the water chemistry types of MSH mining wells, MSH recharge wells and Didu Garden are all Na-Cl type.

As shown in fig. 5, the fingerprint of thermal reservoir fluid in different water samples shows that the content of anions and cations in each well is basically the same, and it is inferred that the hydraulic connection between wells is good.

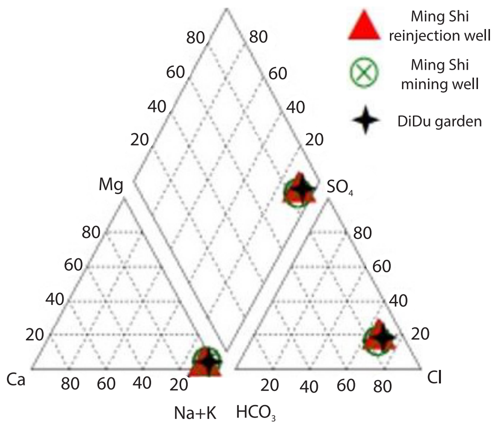

Figure 4. Hydrochemical piper diagram of thermal reservoir fluid in MSH well

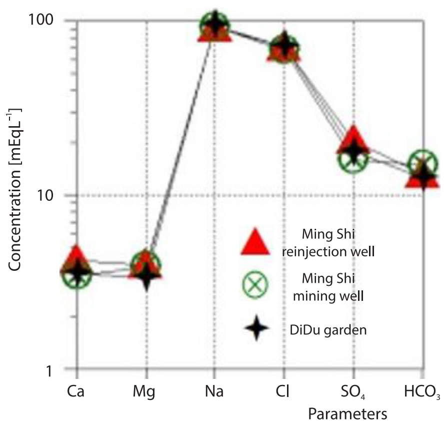

Figure 5. Fingerprint of thermal reservoir fluid in MSH well

Numerical simulation of cycle heat transfer

Numerical model

Taking a mining and irrigation as the modelling research unit, the tail water injection speed is 60 m^3 per hour, 80 m^3 per hour, 100 m^3 per hour, the recharge temperature is 30 °C, and the geothermal energy recovery is 95.4 °C. The model is shown in fig. 6. In the process of simulation, the vertical well type production is adopted, and a quarter of the well pattern is simulated. The length and width of the model are 565.6 m × 565.6 m, respectively, and the model thickness is 1412.8 m. The permeability of each layer is consistent with the previous vertical well model. The horizontal well is located at –1252 m, and the effective thickness of the reservoir in the horizontal section is 3 m, which is in the middle of the reservoir. The length of horizontal section is 500 m, 1000 m, and 1500 m, and the red represents the horizontal section of the horizontal well. According to different flow rates, the migration speed of tab. 6 tail water in 177.8 mm wellbore is obtained.

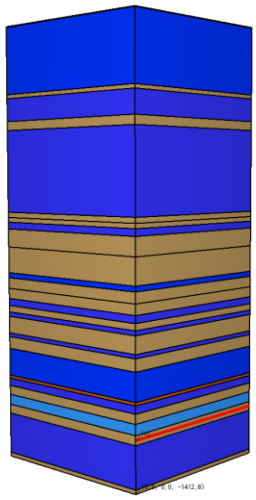

Figure 6. Calculation model of circulating heat exchange horizontal well

Table 6. The 177.8 mm wellbore flow and velocity corresponding table

Flow [m^3 per hour]	60	80	100
Velocity [ms^{-1}]	1.4	1.8	2.3

Simulation results

As shown in fig. 7, the tail water temperature is 30 °C under different flow rates and well spacing conditions. With the increasing of flow rate, the tail water collusion time is faster. When the tail water flow rate is 100 m^3 per hour and the horizontal section distance is 500 m, the wellhead raw water temperature of the production well has dropped to the tail water temperature of the recharge well 30 °C on the 18th day of production. The distance between the production well and the recharge well is certain. The greater the flow rate of tail water recharge is, the faster the tail water is, and the faster the tail water confluence time.

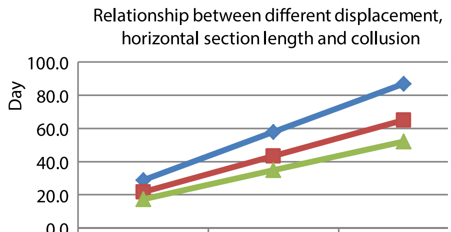

	500 m	1000 m	1500 m
60 m^3/h	28.9	57.9	86.8
80 m^3/h	21.7	43.4	65.1
100 m^3/h	17.3	34.7	52.1

Figure 7. Relationship of circulating time under different flow rates and well spacing

Parameter of well spacing

Figure 8 is the temperature field distribution of the mining area. With the increasing of well spacing, the tail water collusion time becomes shorter. However, combined with the characteristics of loose sandstone formation and poor lithology, increasing the well spacing will greatly increase the risk and cost of horizontal well construction. According to the fluid movement and heat conduction, the mathematical model of reasonable distance between recharge well and production well is established, which provides the basis for determining the reasonable well spacing.

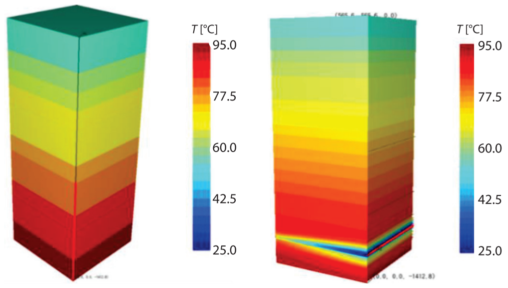

Figure 8. Temperature field distribution of mining irrigation area

Hydrogeology of MSH well area

As shown in fig. 9, two wells are arranged in the target area of 2000 m × 2000 m : MSH mining well and MSH recharge well.

For the strata above 1220.29 m, it can be generalized as a relative aquifuge. The lithology between 1220.29 m and 1415 m is mostly coarse sand and medium coarse sand, which is an aquifer. The depth below 1415 m can be regarded as aquifuge. Therefore, the aquifer group in the study area can be regarded as homogeneous, anisotropic, unstable flow and confined water. The upper boundary of the aquifer is 1220.29 m from the surface, and the lower boundary is 1415 m. The mining irrigation area in this study is generalized as horizontal isotropic, horizontal and vertical anisotropy. The time scale of the study is 30 years, of which the period from November 15 to March 16 is the system operation period, and the rest is the intermittent period. Therefore, the actual operation days of recharge is 10 years. For the spatial distribution of parameters, the discrete parameter generalization method (parameter partition or parameterization) is often used to determine.

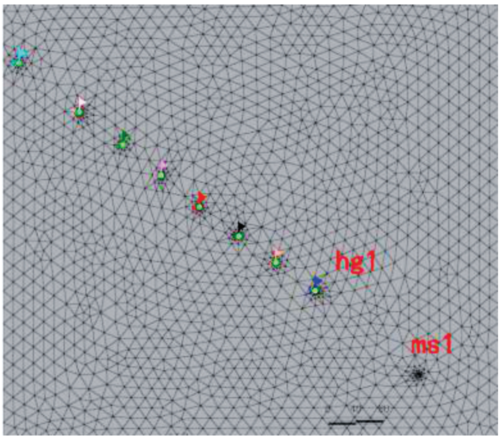

Figure 9. Distribution map and grid subdivision of production and irrigation wells in the study area

Sources and sinks

The source item of this study is MSH recharge well, and the sink item is pumping well Didu Garden and MSH mining well. The simulation test is divided into two parts: pumping test and recharge temperature test:

– The DU production well is a pumping well, pumping water is 1800 m³ per day, wellhead temperature is 52 °C, heat storage temperature is 65 °C, running time is 120 days per year, a total of 30 years.
– The MSH mining wells are pumping wells, wellhead pumping capacity 1320 m³ per day, wellhead temperature 54.5 °C, thermal storage temperature 65 °C. The running time is 120 days/year, a total of 30 years.
– The MSH recharge well, recharge volume is 1560 m³ per day, wellhead temperature is 53 °C, thermal reservoir temperature is 65 °C, operation time is 120 days/year, a total of 30 years.

In simulation, the area parameters are selected according to the geological and hydrogeological conditions of the underground aquifer in the area. The aquifer is set to be homogeneous and isotropic in the horizontal direction. Figure 10 are plane and 3-D maps. Some parameters are shown in tab. 7.

Table 7. Hydrogeological conditions and thermal physical parameters

Parameter name	Aquifer
Depth, H [m]	1220.29~1415
Longitudinal permeability coefficient, K_x [m per day]	1.2757
Transverse permeability coefficient, K_y [m per day]	1.2757
Vertical hydraulic conductivity, K_z [m per day]	0.12757
Water yield, S_y	0.26
Water storage coefficient, S_s	le-5
Partition coefficient, K [Lmg^{-1}]	0.00003
Dispersion, D [m]	10
Effective porosity	0.21
Total porosity	0.35
Supply intensity [mm per year]	15
Evapotranspiration intensity [mm per year]	0
Evaporation critical depth [m]	0
Coefficient of thermal expansion [K]	0
Fluid heat conductivity [Wm^{-1}K^{-1}]	0.65
Solid thermal conductivity [Wm^{-1}K^{-1}]	2.7
Specific heat capacity of liquid [MJm^{-3}K^{-1}]	4.1
Specific heat capacity of medium skeleton [MJm^{-3}K^{-1}]	1.2

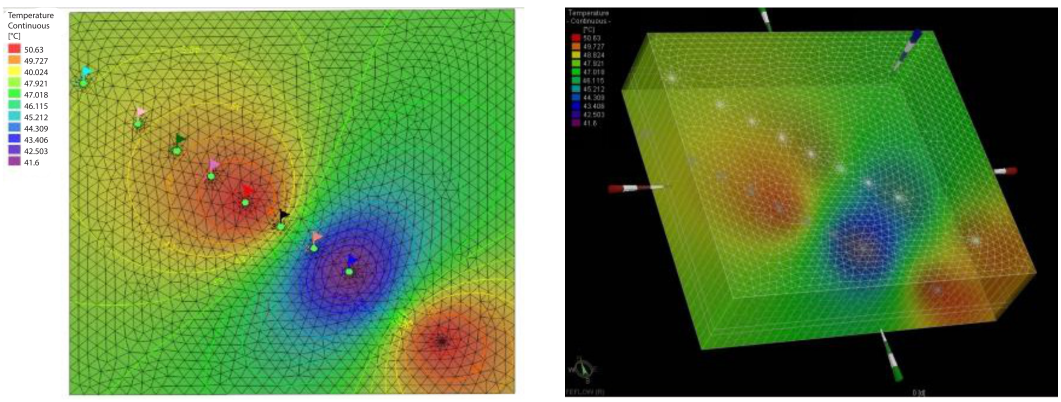

Figure 10. Plan and 3-D map of study area

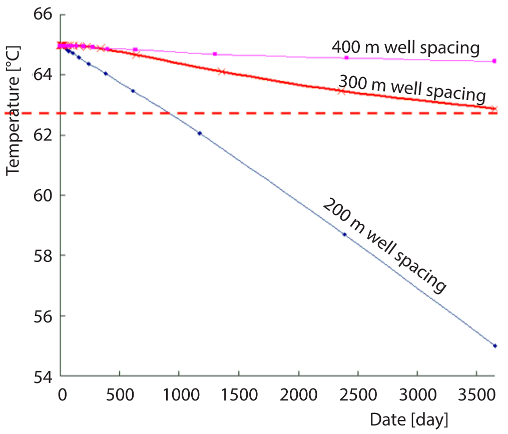

Figure 11. Temperature of mining well under different well spacing conditions

Well spacing simulation results

It can be seen from fig. 11 that under three different well spacing conditions, the temperature change of mining well with recharge of 65 m³ per hour. The greater the distance between the mining well and the irrigation well, the longer the time required for the thermal breakthrough of the mining well, and the smaller the variation of the mining temperature. This is because the farther the distance is, the longer the transfer time from the low temperature area of water injection well to the oil production well, and the smaller the change range of the produced temperature is. In the operation of 30 years, under the premise of preventing the occurrence of thermal breakthrough, mining well distance recharge well reasonable spacing is 300 m. Geothermal tail water recharge is the primary consideration during the recharge operation, the impact on the mining well temperature. It can be seen from the simulation results, recharge 65 m³ per hour, 300 m well spacing, recharge operation 30 years, down less than 2 °C, therefore, a reasonable well spacing is 300 m.

Results and discussions

Dynamic characteristics of natural recharge of MSH well in the first year of heating season

The whole heating season has been recharged for 127 days, November 15-17 is the recovery stage, and it is officially recharged at 10:00 on November 17. The daily reinjection volume is shown in fig. 12, the cumulative reinjection volume reaches 150845 m³, the effective reinjection time is 2694 hours, and the average reinjection volume is 56 m³ per hour. Affected by the heating area, the pumping volume of the production well is limited, so the reinjection volume is relatively low. However, during the reinjection period, the reinjection liquid level of MSH well has not reached the wellhead, and the reinjection volume still has room for improvement. As shown in fig. 13, the maximum instantaneous reinjection volume reaches 82 m³ per hour, and the minimum reinjection volume is as low as 44 m³ per hour. The cumulative recharge-time relationship diagram shows that the recharge volume grows steadily, the aquifer is not blocked, and the reservoir permeability is good.

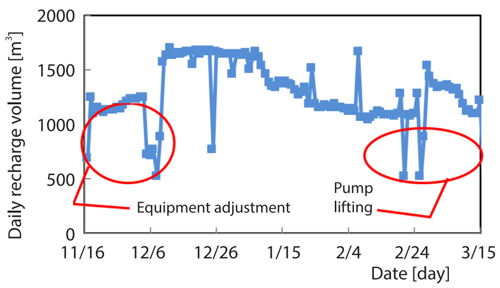

Figure 12. Relationship between daily recharge and time of recharge wells in first heating season

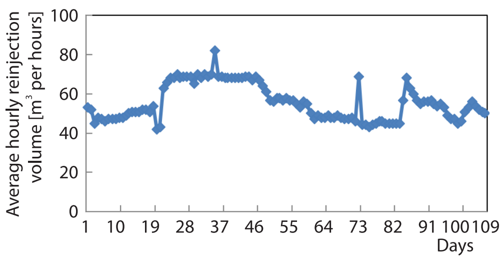

Figure 13. Daily average hourly recharge volume of recharge wells in the first year of heating season

Dynamic characteristics of natural recharge of MSH well in the second heating season

The MSH recharge test is to recharge the MSH recharge well after pumping heat from the MSH exploration well. The daily recharge amount is shown in fig. 14. Figure 15 shows that the total recharge of the project is 111125 m^3 per hour, and the effective recharge time is 2009 hours. As shown in fig. 16, the average recharge is 55.3 m^3 per hour and the maximum is 68.7 m^3 per hour. However, after long-term reinjection, the reinjection volume decreases and the reinjection pressure increases. After 25 hours of pump lifting, the reinjection effect is not good. After a long time of pump lifting, the reinjection volume is stable at about 50~55 m^3 per hour.

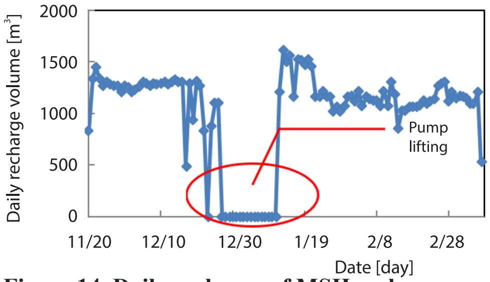

Figure 14. Daily recharge of MSH recharge wells in the second year of heating season

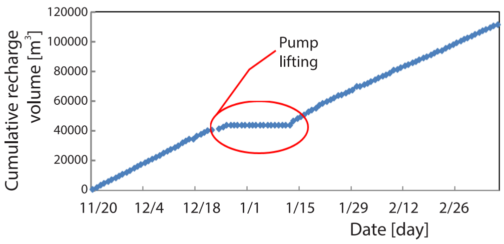

Figure 15. Cumulative recharge of MSH recharge wells in the second heating season

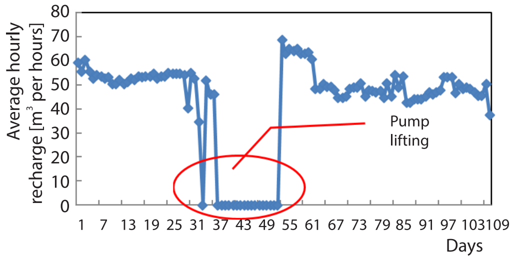

Figure 16. Hourly recharge of MSH recharge wells in the second heating season

Conclusion

The geological sedimentary environment of Leling is stable, and the Neogene sandstone thermal reservoir with unimpeded water fault is favorable for recharge. Through the analysis of water chemistry, the recharge of the same layer in this area can effectively reduce the probability of chemical blockage. The recharge of different water quality in different layers increases the probability of chemical blockage and reduces the recharge effect. In the injection-production system, with the increase of the flow rate, the tail water collusion time is faster. When the tail water flow rate is 100m^3 per hour and the horizontal section distance is 500 m, the wellhead raw water temperature of the production well has dropped to the tail water temperature of the recharge well 30 °C on the 18th day of production. When the reinjection volume of the reinjection well is 65m^3 per hour, the greater the distance between the production well and the injection well, the longer the time required for the thermal breakthrough of the production well, and the smaller the change range of the mining temperature. The reasonable well spacing of the production well is 300 m. After two heating seasons of geothermal reinjection field test, the reinjection rate of MSH reinjection well is 100%, the maximum reinjection volume is 82 m^3 per hour, and the reinjection operation is stable. It shows that the physical properties and water quality characteristics of sandstone thermal reservoir in Leling area meet the conditions of sandstone reinjection, and the reinjection effect is good, which ensures the stable pressure of the reservoir.

Acknowledgment

This research work was supported by Key R and D Plan of Sichuan Province (23ZDYF2302).

References

[1] Zhang, W., *et al*., Characteristics Ofgeothermal Resources in Sedimentarybasins, *Geology in China*, 6 (2019), 2, pp. 255-268
[2] Pang Z., *et al*., State-of-the-Art of the Geothermal Industry, *China Nuclear Industry*, (2017), 12, pp. 47-50
[3] Song X., *et al.*, Laboratory-Scale Experimental Study on the Injection-Production Performance of a Multilat-Eral-Well Enhanced Geothermal System, *Petroleum Drilling Techniques*, *49* (2021), 1, pp. 81-87
[4] Li, X., *et al*., Analysis on Ththermal Efficiency Improvement Process for Geothermal Well in Porous Sandstone, *Oil Drilling and Production Technology*, *39* (2017), 4, pp. 484-490
[5] Mei, B., *et al*., The Technology and Application of Water Recharge in the Tail Water of Geothermal Well, *China Resources Comprehensive Utilization*, *36* (2018), 1, pp. 167-169
[6] Cao, Q., *et al*., Development Status Ofgeothermal Reinjection at Home and Abroad and Its Enlightenment, *Oil Drilling and Production Technology*, *43* (2021), 2, pp. 203-211
[7] Luo, T., Study on Water Injection Capacity of Recharge Well for Thermal Recovery, *Sino-Global Energy*, *24* (2019), 6, pp. 21-25
[8] Zhang, H., A Well Pattern Evaluation Method for Geothermal Resource Recycling-a Case Study of Geothermal Field in the Central Uplift Belt of Dongying Sag, *Petroleum Geology and Recovery Efficiency*, *24* (2017), 1, pp. 86-91
[9] Liang, H., *et al*., Scaling Spot Prediction and Analysis of Influencing Factors for a Geothermal Well in Boye County, Hebei Province, *Petroleum Drilling Techniques*, *48* (2020), 5, pp. 105-110
[10] Fu, Y., *et al.*, Present Situation and Prospect of Hot Dry Rock Exploration and Development, *Oil Drilling and Production Technology*, *40* (2018), 4, pp. 526-540
[11] Mcdowell-Boyer, L. M., *et al*., Particle Transport through Porous Media, *Water Resources Research*, 22 (1986), 13, pp. 1901-1921
[12] Rehg, K. J., *et al*., Effects of Suspended Sediment Characteristics and Bed Sediment Transport on Stream-Bed Clogging, Hydrological Processes, *An International Journal*, *19* (2005), 2, pp. 413-427
[13] Juerg, M., *et al*., Rapid Carbon Mineralization for Permanent Disposal of Anthropogenic Carbon Dioxide Emissions, *Science*, *352* (2016), 6291, pp. 1312-1314
[14] Wang, G., *et al*., Numerical Simulation of Geothermal Abandoned Water Recharge in Xi ‘an Geothermal Field, *Earth*, *23* (2002), 2, pp. 183-188
[15] Ding, H., *et al*., Geothermal Development and Recharge in Xianyang City, *Shanxi Architecture*, *36* (2010), 35, pp. 164-165
[16] Zarrouk, S., *et al*., A Review of Worldwide Experience of Reinjection in Geothermal Fields, *Proceedings*, 28th NZ Geothermal Workshop, Auckland, New Zealand, 2006
[17] Stein, P. C., *A Study of the Theory of Rapid Sand Filtration of Water through Sand*, Massachusetts Institute of Technology, Massachusetts, Mass., USA, 1940
[18] Xu, T., Pruess, K., Numerical Simulation of Injectivity Effects of Mineral Scaling and Clay Swelling in a Fractured Geothermal Reservoir, *Proceedings*, Transactions-Geothermal Resources Council, Palm Springs, Cal., USA, 2004, Vol. 28, pp. 1-14
[19] Rivera, D. A., *et al*., Reinjection in Geothermal Fields − A Worldwide Review Update, *Renewable and Sustainable Energy Reviews*, *53* (2016), Jan., pp. 105-162
[20] Settari, A., Walters, D. A., Advances in Coupled Geomechanical and Reservoir Modelling with Applications to Reservoir Compaction, *Spe Journal*, 6 (2001), 3, pp. 334-342
[21] Tran, D., *et al*., New Iterative Coupling between a Reservoir Simulator and a Geomechanics Module, *SPE Journal*, *9* (2004), 03, pp. 362-369
[22] LI, H., *et al*., Soil Bacterial Communities of Different Natural Forest Types in Northeast China, *Plant and Soil*, *83* (2014), 1/2, pp. 203-216
[23] Alain, K., Querellou, J., Cultivating the Uncultured: Limits, Advances and Future Challenges, *Extremophiles*, *13* (2009), 4, pp. 583-594
[24] Knowles, P., *et al*., Clogging in Subsurface-Flow Treatment Wetlands: Occurrence and Contributing Factors, *Ecological Engineering*, *37* (2011), 2, pp. 99-112
[25] Thullner, M., Comparison of Bioclogging Effects in Saturated Porous Media within One-and 2-D Flow Systems, *Ecological Engineering*, *36* (2010), 2, pp. 176-196

Paper submitted: October 3, 2022
Paper revised: November 2, 2022
Paper accepted: November 21, 2022